

Review

Breaking biological symmetry in membrane proteins: The asymmetrical orientation of PsaC on the pseudo- C_2 symmetric Photosystem I core

B. Jagannathan^a and J. H. Golbeck^{a, b, *}

^a Department of Biochemistry and Molecular Biology, ^b Department of Chemistry, The Pennsylvania State University, University Park, PA 16802 (USA), Fax: 1 814 863 7024, e-mail: jhg5@psu.edu

Received 22 October 2008; received after revision 17 November 2008; accepted 05 December 2008
Online First 13 January 2009

Abstract. The elucidation of assembly pathways of multi-subunit membrane proteins is of growing interest in structural biology. In this study, we provide an analysis of the assembly of the asymmetrically oriented PsaC subunit on the pseudo C_2 -symmetric Photosystem I core. Based on a comparison of the differences in the NMR solution structure of unbound PsaC with that of the X-ray crystal structure of bound PsaC, and on a detailed analysis of the PsaC binding site surrounding the F_X iron-sulfur cluster, two models

can be envisioned for what are likely the last steps in the assembly of Photosystem I. Here, we dissect both models and attempt to address heretofore unrecognized issues by proposing a mechanism that includes a thermodynamic perspective. Experimental strategies to verify the models are proposed. In closing, the evolutionary aspects of the assembly process will be considered, with special reference to the structural arrangement of the PsaC binding surface.

Keywords. PsaC, Photosystem I, C_2 -symmetry, PsaD, stromal proteins, reaction center, iron-sulfur cluster.

Introduction

Photosynthesis is the process in which sunlight is captured and converted into chemical bond energy by plants, algae and photosynthetic bacteria. The basic reaction involves the light-driven transfer of electrons across the photosynthetic membrane, generating an electrochemical gradient that is subsequently used for carbon fixation. Oxygenic photosynthetic organisms, including cyanobacteria, algae and plants, are capable of splitting water to extract electrons, liberating oxygen as a by-product. Anoxygenic phototrophs such as purple bacteria and green sulfur bacteria

derive their electrons from organic and inorganic molecules and hence do not evolve oxygen. Oxygenic photosynthesis is driven by two protein-pigment complexes termed reaction centers (RCs). Photosystem II operates at the oxidizing end of the redox scale and incorporates the water-splitting manganese enzyme that extracts electrons from water. The electrons are subsequently transferred to Photosystem I (PS I) via a membrane-bound cytochrome b_6f complex. PS I operates at the reducing end of the redox scale and catalyzes the reduction of $NADP^+$ to $NADPH$, thereby generating the reducing equivalents that are required for carbon fixation.

* Corresponding author.

Photosystem I

PS I is a membrane-bound protein-pigment complex that contains pigment molecules to absorb light energy and redox cofactors to carry out trans-membrane electron transfer. A model based on the 2.5 Å resolution X-ray crystal structure of the trimeric PS I reaction center from the cyanobacterium, *Thermosynechococcus elongatus* (PDB ID 1JB0) has provided invaluable structural information on the three-dimensional arrangement of the pigments, proteins and cofactors (Fig. 1) [1]. Each monomer of the cyanobacterial PS I complex contains 12 protein subunits, 96 chlorophyll *a* (Chl *a*) molecules, 22 carotenoids, four lipids, two phylloquinones and three [4Fe-4S] clusters. PsaA (83 kDa) and PsaB (83 kDa) form the heterodimeric core and contain the majority of the antenna molecules and redox cofactors. PsaC (9 kDa) is a membrane-extrinsic (stromal) subunit that contains the two terminal electron acceptors in the electron transfer chain. PsaD (15 kDa) and PsaE (8 kDa) are stromal subunits and, along with PsaC, provide a docking site for the soluble electron acceptors ferredoxin and flavodoxin [2, 3]. Cyanobacterial PS I contains seven additional subunits (PsaF, PsaI, PsaJ, PsaK, PsaL, PsaM and PsaX) whose roles are not well established. Some, including PsaJ, PsaK, PsaL, PsaM and PsaX, function as additional antenna proteins by binding Chl *a* molecules [4]. Others, such as PsaL [5, 6], along with PsaI [7, 8], contribute to the trimerization of cyanobacterial PS I.

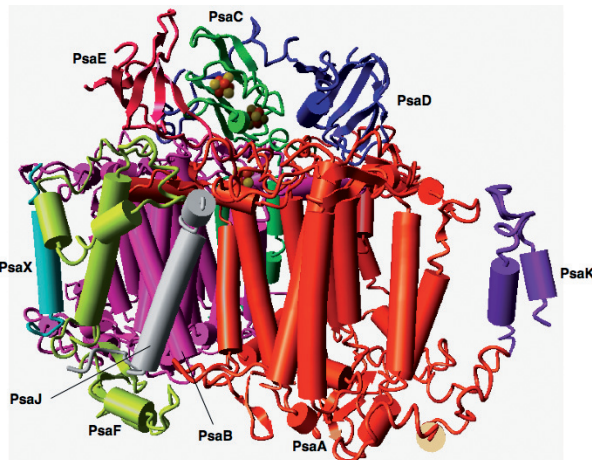


Figure 1. Side view of the arrangement of all proteins in one monomer of PS I (PDB ID: 1JB0), with the main subunits indicated.

The electron transfer chain starts at a special pair of Chl *a* molecules termed P₇₀₀, named for its peak absorbance in the visible region. When P₇₀₀ becomes

excited to the singlet state, its electron is transferred to A₀, a Chl *a* monomer. An additional molecule of Chl *a* (A) is located between P₇₀₀ and A₀, and may act as an electron transfer intermediate [4]. The initial P₇₀₀⁺A₀⁻ charge-separated state is stabilized by rapid transfer of the electron to a bound phylloquinone, A₁ and then to a series of [4Fe-4S] clusters, termed F_X, F_A and F_B [9]. The latter function as an electron transfer wire, shuttling the electron to the stromal surface and making it available to ferredoxin or flavodoxin. The terminal acceptors, F_A and F_B are located in the PsaC subunit. Because the terminal electron acceptors are iron-sulfur clusters, and because the core is composed of the PsaA/PsaB subunits, PS I is termed a heterodimeric Type I RC.

This article will focus on the assembly of the stromal subunits and, in particular, on the final steps in the association of the PsaC subunit with the membrane-bound PS I core. Based on a comparison of the NMR solution structures of unbound PsaC and the X-ray crystal structure of bound PsaC, and on a detailed analysis of the PsaC binding region on the PsaA/PsaB surface, two models can be envisioned for the assembly of PsaC onto the PS I core. Both models will be described in detail, and their strengths and weaknesses will be addressed in the context of a thermodynamic perspective. Experimental strategies to verify these models will also be discussed. Finally, the evolutionary aspects of the assembly process will be considered, with special reference to the structural changes in the PsaC binding surface.

Symmetry Elements in the PsaA/PsaB Heterodimer

The overall symmetry within the PsaA/PsaB heterodimer is evident even in a cursory analysis of the amino acid sequences of the protein subunits. PsaA and PsaB in *Thermosynechococcus elongatus* contain an almost identical number of amino acids and have comparable molecular masses. Although there are certain differences in the amino acid sequences, particularly in N-terminal half of the protein associated with the light-harvesting chlorophylls, there is a high degree of similarity in the C-terminal half of the protein in the vicinity of the redox cofactors. For instance, the F_X iron-sulfur cluster is ligated by two cysteines each from PsaA and PsaB [10, 11, 12], which are located in homologous regions on each subunit. The 2.5 Å resolution crystal structure of PS I further reinforces the high degree of symmetry within the PsaA/PsaB heterodimer [1]. Each subunit is comprised of 11 transmembrane α -helices that are connected via loop regions on the stromal and luminal surfaces. The symmetry between PsaA and PsaB

becomes highest in the environment surrounding the redox cofactors. The primary donor, P_{700} , is comprised of a Chl a molecule coordinated by a His residue on PsaB and a Chl a' molecule (the C13² epimer of Chl a) coordinated by a homologous His residue on PsaA [13]. According to the currently accepted paradigm, this 'special pair' becomes excited to its singlet state due to the absorption of light, and it transfers an electron to the primary acceptor A_0 via the bridging Chl a molecule, A [9]. An alternate mechanism for initial charge separation has also been proposed in which the bridging Chl a molecule, A, functions as the primary electron donor and the A_0 Chl a molecule is the primary electron acceptor [14].

The organic cofactors of the electron transport chain (A, A_0 and A_1) are arranged in two symmetric branches along the PsaA and PsaB subunits. An axis of symmetry passes through the center of P_{700} as well as through the center of the F_X cluster. The two branches of electron transfer are also in nearly perfect symmetry; the inter-cofactor distances are very nearly identical in both of the branches [1], and the cofactors in each of the branches are located at almost equal distances from the PsaA/PsaB interface (Fig. 2). The symmetry that is observed in the PS I heterodimer is known as C_2 -symmetry; if the PsaA/PsaB complex were to be rotated by 180° around this interface, the resulting geometric orientation would be identical to the orientation prior to rotation. Nevertheless, the PsaA and PsaB subunits are not precisely identical, and the system is best regarded as pseudo C_2 -symmetric. The degree of symmetry weakens as one moves farther away from the electron transport cofactors; however, even in the distal regions, the PsaA/PsaB heterodimer still maintains a fair degree of overall symmetry.

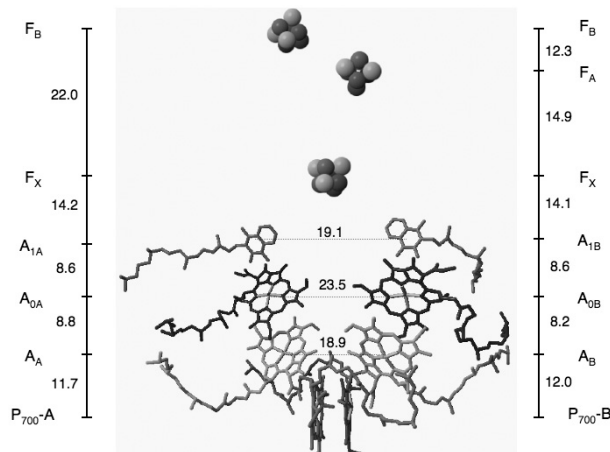


Figure 2. The arrangement of redox cofactors in PS I with center-to-center distances (in Å) (PDB ID: IJB0).

The presence of two branches of electron transfer cofactors begs the question as to whether both branches support electron transfer during photosynthesis. It appears that the pathway chosen by the electron depends somewhat on the species. Among the limited number of species studied, electron transfer is strongly biased towards the PsaA-side branch of cofactors in cyanobacterial PS I [15, 16], whereas the electron flow is almost equally divided between both the branches in algal PS I [17, 18, 19].

The two branches of redox cofactors converge at the F_X cluster and subsequent electron transfer through the F_A and F_B clusters is linear. The strong symmetry within the early electron transport chain is broken by the stromal subunits, especially PsaC. Although PsaC binds in the center of the C_2 -symmetry axis above the F_X binding site, the F_A and F_B iron-sulfur clusters are located at different distances from F_X and from the nearest symmetry-related phylloquinone in either the PsaA or PsaB binding pocket [1]. PsaD binds to the stromal interface with its N-terminus positioned above the C-terminus of PsaC. A clamp-like arm of polypeptide wraps over PsaC, leaving the C-terminus of PsaD attached to the PsaB subunit. The smallest stromal protein, PsaE binds adjacent to the C-terminus of PsaD. Thus, PsaC is flanked on either side by the PsaD and PsaE subunits on the stromal surface of PS I.

Assembly of the stromal subunits in Photosystem I

The assembly of the stromal subunits has been extensively studied using both biochemical and spectroscopic techniques. PsaC, PsaD and PsaE can be dissociated from the PS I complex by treatment with high concentrations of chaotropes such as urea, sodium thiocyanate, or sodium iodide [20]. The addition of a chaotropic agent likely causes disruption of the tertiary structure of the stromal proteins, leading to their dissociation. Since the [4Fe-4S] clusters, F_A and F_B are located in PsaC, they are also lost, thus disrupting the electron transfer chain. The chaotropic-treated PS I complexes contain F_X as the terminal electron acceptor and are termed $P_{700}-F_X$ cores. The *psaC*, *psaD* and *psaE* genes have been cloned in *Escherichia coli* [21, 22] and hence it is possible to obtain unbound, recombinant stromal proteins for detailed study. It is possible to insert the two [4Fe-4S] clusters in unbound, recombinant apo-PsaC by chemical reconstitution with iron and inorganic sulfide under reducing conditions [23]. The resulting holo-PsaC is able to rebind to $P_{700}-F_X$ cores in the absence of chaperones or added sources of energy, and thus restore electron transfer to the F_A and F_B

clusters [23]. The binding can be tracked by spectroscopic techniques that monitor the charge recombination kinetics between P_{700}^+ and the terminal electron acceptor. It is relatively straightforward to observe the order of magnitude difference between the charge recombination in $P_{700}\text{-}F_X$ cores (~ 1 ms) and $P_{700}\text{-}F_A/F_B$ complexes (~ 100 ms) [9]. The ability of recombinant PsaC, PsaD and PsaE to bind to $P_{700}\text{-}F_X$ cores *in vitro* suggests that the latter are fully assembled. It is thus likely that the membrane intrinsic portion of PS I is assembled first, followed by the binding of the stromal subunits.

The $P_{700}\text{-}F_X$ cores can be degraded further by the addition of urea in the presence of an oxidant such as $\text{K}_3\text{Fe}(\text{CN})_6$, which results in the denaturation of the F_X cluster [24]. These preparations are termed $P_{700}\text{-}A_1$ cores. PsaC is unable to bind to $P_{700}\text{-}A_1$ cores, which indicates that the presence of F_X is required for PsaC to bind. An *in vivo* cyanobacterial mutant lacking the *rubA* gene, which is involved in the assembly of the F_X cluster, was found to be devoid also of PsaC, PsaD and PsaE [25], a finding consistent with the *in vitro* studies. The [4Fe-4S] clusters, F_A and F_B , become singly reduced and paramagnetic upon reduction and can be detected around $g = 2$ by EPR spectroscopy. The magnetic properties of F_A and F_B are strongly dependent on their environment; a slight change causes a significant alteration in their EPR spectra. For example, the addition of PsaC to $P_{700}\text{-}F_X$ cores leads to changes in the EPR spectrum of F_A and F_B , which is indicative of a modification in the environment surrounding the iron-sulfur clusters [26]. The addition of recombinant PsaD to $P_{700}\text{-}F_X\text{/PsaC}$ complexes leads to further changes in the EPR spectrum of F_A and F_B [26]. The EPR spectrum of $P_{700}\text{-}F_X\text{/PsaC/PsaD}$ complexes is identical to intact PS I complexes, indicating that PsaC has attained its native orientation. The addition of PsaE to $P_{700}\text{-}F_X\text{/PsaC/PsaD}$ complexes does not induce further alterations in the EPR spectrum of F_A or F_B and it is likely that it does not play a role in the assembly of PsaC [26]. Thus, it is possible to observe the three stages of PsaC assembly by monitoring the EPR spectrum of F_A and F_B : unbound PsaC, $P_{700}\text{-}F_X\text{/PsaC}$ complexes and $P_{700}\text{-}F_X\text{/PsaC/PsaD}$ complexes.

The study of *in vivo* *psaC*, *psaD* and *psaE* deletion mutants provide further information on the stromal assembly process. The *in vivo* *psaC* deletion mutant does not contain bound PsaD [27], which is consistent with the conclusion that a $P_{700}\text{-}F_X\text{/PsaC}$ complex is a prerequisite for PsaD to bind. As expected, the *in vivo* *psaD* deletion mutant contains bound PsaC [28]. The magnetic properties of F_A and F_B in *psaD* deletion variants are identical to *in vitro* prepared $P_{700}\text{-}F_X\text{/PsaC}$ complexes, implying that the *in vitro* binding proce-

dure is identical to the *in vivo* stromal assembly process. The *psaE* deletion mutant still retains PsaC and PsaD [22], confirming that the assembly of PsaC and PsaD does not require the presence of PsaE. It is also consistent with the *in vitro* studies of $P_{700}\text{-}F_X\text{/PsaC/PsaD}$ complexes, which show an EPR spectrum of F_A or F_B identical to the wild-type [26]. PsaE may have multiple roles; it may assist in the docking of the soluble electron acceptor proteins, ferredoxin and flavodoxin [29], and it may be involved in the cyclic electron transfer pathway around PS I [30]. The presence of bound PsaD also appears to be required for the stable assembly of PsaE. PsaE incorporated into the wild-type membranes was resistant to treatment with chaotropic agents and to proteolytic digestion, but the absence of PsaD caused PsaE to be removed by these treatments [31]. PsaE incorporated into membranes of a *psaD/psaF/psaJ* deletion strain was susceptible to removal by chaotropic agents and proteolytic digestion, suggesting that PsaF and PsaJ may also interact with PsaE and serve to stabilize this PS I subunit.

Given the experimental evidence, it appears that the stromal subunits in PS I are assembled in a well-defined order: PsaC first, followed by PsaD and then PsaE. A PsaC/PsaD/PsaE pre-complex has never been observed; hence, there is no indication that the stromal subunits associate with each other prior to binding on the PsaA/PsaB heterodimer surface.

The Binding Site of PsaC on Photosystem I

The structural design principles of a photosynthetic reaction center involve close placement of the redox cofactors. This is necessary to support electron transfer among successive cofactors at rates faster than the charge recombination between the electron donor (P_{700}^+) and the preceding cofactor. In PS I, the rates of forward electron transfer are usually three orders of magnitude greater than that of charge recombination with the preceding acceptor, ensuring a quantum yield close to 1.0. However, the presence of the terminal electron acceptors, F_A and F_B , on a separate, membrane extrinsic subunit, PsaC, poses an interesting design problem. The distance between the membrane intrinsic cofactor, F_X and the membrane extrinsic cofactor, F_A needs to be short enough to support a fast rate of electron transfer. Further, the PsaC-PsaA/PsaB interface needs to be well shielded from oxygen; else the electron might be donated to O_2 after it reaches F_X . In addition to lowering the intrinsic quantum yield, the reduction of O_2 results in the formation of reactive oxygen species such as superoxide (O_2^-) and hydroxy (OH^-) radicals that are

potentially lethal to the cell. An inspection of the PS I crystal structure shows that F_x and F_A are located ~ 15 Å (center to center) from each other and that PsaC is attached to PsaA/PsaB via 10 ionic bonds and five hydrogen bonds [32]. The presence of such a large number of binding contacts between PsaC and the PS I core may be to ensure that the association is extremely tight and that the binding interface is inaccessible to solvent and/or oxygen. The high concentrations of chaotropic agents required to dissociate PsaC from PS I further highlights the tight binding between the protein subunits [20].

To achieve the closest possible distance between F_x and F_A , PsaC binds directly above the F_x binding site near the center of the pseudo C_2 -symmetry axis, with the F_A cluster being proximal to F_x . The ligating Cys residues are part of highly conserved loop regions that connect the transmembrane α -helices h and i in both PsaA and PsaB (Fig. 3). The loop regions have multiple roles; in addition to coordinating F_x , they also appear to shield the iron-sulfur cluster from dioxygen. A [4Fe-4S] cluster is comprised of covalently linked iron and sulfur atoms. During oxidative denaturation, the bridging sulfides (S^{2-}) become oxidized to the elemental S^0 state and a persulfide bridge is formed between the cysteine residues, causing the rapid degradation of the cluster [33]. A well-protected environment around F_x is therefore critical for stability, particularly during the stromal assembly process. Since P_{700} - F_x cores are putative intermediates in the assembly of PS I, the stability of F_x is paramount. The excellent shielding of F_x by the loop regions is evidenced by the high stability of P_{700} - F_x cores prepared *in vitro* by removal of PsaC or *in vivo* by genetic deletion of the *psaC* gene [20, 27].

The F_x -coordinating loops and the stromal loop of helices h and i contain Asp residues that are involved in the formation of the 10 ionic bonds with PsaC. Asp568 and Asp579 on PsaA (D_{568A} and D_{579A}) form ionic bonds with Arg52 (R_{52C}) on PsaC; Asp555 and Asp566 on PsaB (D_{555B} and D_{566B}) form ionic bonds with Lys51 and Arg65 (K_{51C} and R_{65C}) on PsaC (Fig. 4). These Asp residues share the strong C_2 -symmetry that is observed around the preceding redox cofactors: they are located at identical positions in the loop regions of the PsaA and PsaB subunits and provide a symmetric binding platform for PsaC.

Unlike the perfectly symmetric docking surface on PsaA/PsaB, the bonding Arg residues on PsaC are derived from very different structural elements: R_{52C} is adjacent to the F_A -coordinating C_{53C} and at the start of an α -helical turn that connects F_A and F_B , and R_{65C} is located on the final β -strand of PsaC. K_{51C} and R_{52C} are part of the F_A cluster coordinating CxxCxxCxxxCP motif, whereas R_{65C} is part of the pre-C-terminus that

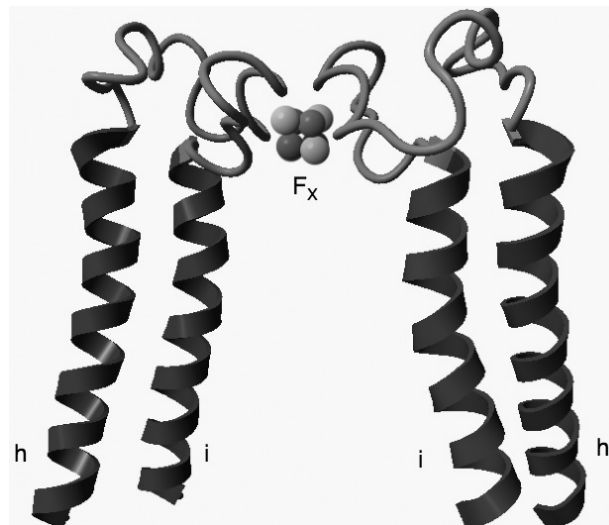


Figure 3. A closer view of the loop regions that connect transmembrane helices h and i on PsaA (A-hi) and PsaB (B-hi) (PDB ID: 1JB0). The loops contain the Cys residues that coordinate the F_x cluster and also provide the Asp residues that form symmetric ionic bonds with PsaC.

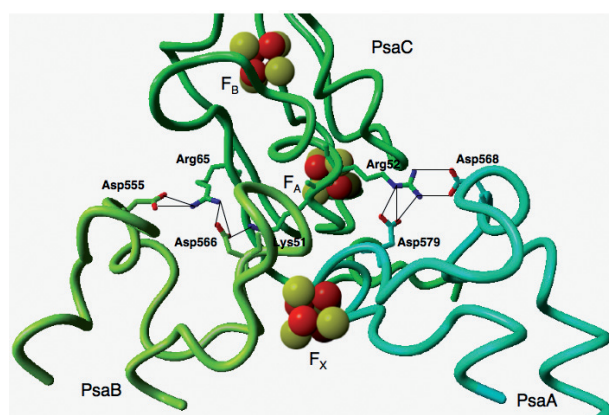


Figure 4. The symmetric network of ionic bonds between PsaC and PsaA/PsaB. (PDB ID: 1JB0).

forms an antiparallel β -sheet with the N-terminus in the bound form of PsaC. In spite of these differences, the network of ionic PsaC-PsaA contacts appears identical to the ionic PsaC-PsaB contacts. R_{52C} forms five ionic bonds with D_{568A}/D_{579A} and K_{51C}/R_{65C} form five ionic bonds with D_{555B}/D_{566B} . The equal division of ionic contacts between PsaA and PsaB represents a symmetric and stable binding surface for PsaC. The arrangement of ionic contacts reflects the overall design philosophy of the PS I stromal binding surface. The placement of K_{51C} and R_{52C} in the F_A -ligating cysteine motif and the location of the PsaA/PsaB Arg residues in the F_x -coordinating loops ensure that F_x and F_A are positioned in closest proximity to each other, thus enabling the fastest possible rate of forward electron transfer. Given the strict relationship

between distance and electron transfer rate described by Marcus theory [34], an increase in the F_x - F_A distance by a few Å could be enough to make the rate of forward electron transfer competitive with wasteful charge recombination between $P700^+$ and the preceding acceptor.

PsaC also forms three hydrogen bonds with the PS I core in a region distant from the symmetric ionic contacts. These bonds are formed between $T73_C/Y80_C$ on the C-terminus of PsaC and $Q678_B/K702_B/P703_B$ on PsaB (Fig. 5). However, unlike the symmetric ionic contacts, a symmetry-related network of H-bonds does not exist on the PsaA subunit. Thus, the three H-bonds between the C-terminus of PsaC and PsaB are highly specific and are likely the key to the asymmetric binding of PsaC (see below).

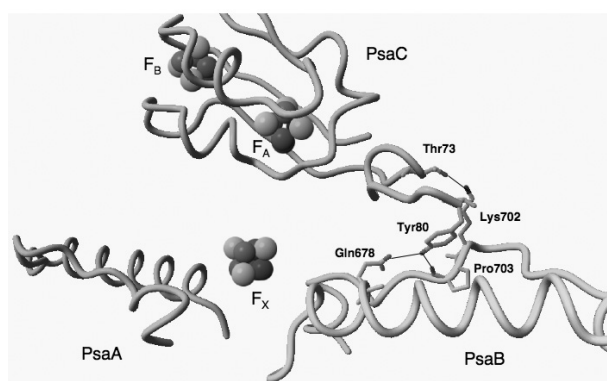


Figure 5. The symmetry-breaking hydrogen bonds between PsaB and the C-terminus of PsaC. (PDB ID: 1JB0).

The binding region of PsaC on the PS I stromal surface presents a case of progressive diminution of biological symmetry with distance. The binding surface presented by the F_x -coordinating loops on PsaA/PsaB is perfectly C_2 -symmetric; the PsaC-PsaA/PsaB ionic contacts weaken the symmetry since the bonding Arg residues on PsaC originate from different structural elements; and the specific H-bonds between PsaB and the C-terminus of PsaC completely break the symmetry of the PsaC binding region on the PS I stromal surface.

The Two Possible Orientations of PsaC on the PS I Core

The high degree of C_2 -symmetry observed at the PsaC docking site poses a problem in terms of the conformational dynamics encountered during the assembly process. Because the arrangement of the bonding Asp residues on PsaA/PsaB is highly symmetric, the question arises as to how PsaC is able to distinguish

between the Asp residues on PsaA and the Asp residues on PsaB during assembly. In other words, why does $R52_C$ bind only to $D568_A/D579_A$ (PsaA) and not to $D555_B/D566_B$ (PsaB)? Similarly, $K51_C$ and $R65_C$ only form bonds with $D568_A/D579_A$ (PsaA) instead of $D555_B/D566_B$ (PsaB). If the network of ionic bonds were to be interchanged from the PsaA side to the PsaB side and vice versa, the resulting orientation of PsaC could be rotated 180° from its native orientation. A detailed analysis of the X-ray crystal structure of PS I confirms the potential ambiguity in specifying the orientation of PsaC during stromal assembly. If the bound PsaC subunit is rotated by 180° around the C_2 -symmetric axis on PS I, the α -carbons of $R52_C$ and $R65_C$ are found to overlay perfectly [32]. Thus, $R52_C$ will form bonds with $D555_B/D566_B$ (PsaB) and $R65_C$ will form bonds with $D568_A/D579_A$ (PsaA). $K51_C$ will switch its single bond from $D566_B$ to $D579_A$. Clearly, a similar network of symmetric ionic contacts will be established if PsaC binds in the rotated orientation. This means that during assembly, PsaC must be able to choose between the correct orientation, in which the F_A - F_B connecting vector is pointing to toward PsaX, and the 180°-rotated orientation in which the F_A - F_B connecting vector is pointing toward PsaK (Fig. 6). Yet, both orientations are equally possible, given that the network of ionic contacts is C_2 -symmetric.

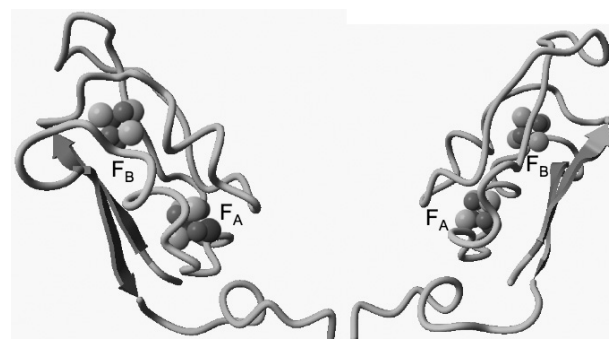


Figure 6. Structural depiction of the correct (left) and 180°-rotated (right) orientations of PsaC on the PS I core (PDB ID: 1JB0).

The specific H-bonds between PsaB and the C-terminus of PsaC, however, have no symmetry related counterpart on PsaA. $T73_C$ and $Y80_C$ cannot form H-bonds with $P719_A/Q718_A$, the corresponding amino acids on PsaA. If PsaC were to be rotated by 180° around the PsaA/PsaB C_2 -symmetry axis, there would be a number of 'clashes' between the surface helix (A-jk) of PsaA and the C-terminus of PsaC. To avoid these clashes, the C-terminus of PsaC would need to assume a different conformation from that of the non-rotated form. Given the presence of these symmetry-breaking elements, the question arises as to how PsaC

locates these elements and docks in a single orientation on the P_{700} - F_X core on the PsaA/PsaB heterodimer. Before we delve into this issue, it is essential to describe the role of the PsaD subunit and to compare the structures of PsaC in the unbound and bound forms.

The Role of PsaD in Stromal Assembly

The PsaD subunit adjoins PsaC on the stromal surface and has extensive interactions with PsaC and the PsaA/PsaB heterodimer. The N-terminus of PsaD covers the surface of the symmetry-breaking binding site of the C-terminus of PsaC and it forms multiple contacts with PsaA and PsaB [1]. The C-terminus of PsaD wraps around the stromal-facing surface of PsaC and attaches to the stromal interface of PsaB above the stromal loops of helices i/h and h/g. The 'C-clamp' of PsaD likely stabilizes the PsaC subunit and additionally serves to define the binding site for ferredoxin and flavodoxin.

If PsaC and PsaD were to be rotated together by 180° around the C_2 -symmetry axis, only one-third of the contacts between PsaD and PsaA/PsaB would exist when compared to the contacts between non-rotated PsaD and PsaA/PsaB [32]. It is therefore unlikely that PsaD will bind to the P_{700} - F_X /rotated PsaC complex, given that it will lose two-thirds of its contacts with PsaA/PsaB. As a result, the binding of PsaD introduces a high degree of preference for assembling the stromal ridge structure with correctly oriented PsaC. The binding of PsaD is also functionally relevant; F_A and F_B attain their final magnetic properties only after PsaD binds [26], and only with PsaD bound are F_A and F_B able to reduce ferredoxin [29].

In principle, the binding of PsaD could provide the driving force for the correct assembly of PsaC since it introduces a high degree of orientational specificity. However *in vitro* resolution/reconstitution and *in vivo* genetic deletion studies clearly show that the presence of bound PsaC on the PS I core is a prerequisite for the binding of PsaD [26, 27]. As a result, PsaC must attain its orientation without any assistance from PsaD. Considering only the region of PsaC that binds above the PS I axis of symmetry, there is a 50% probability that PsaC will bind to the P_{700} - F_X core in the correct orientation and a 50% probability that PsaC will bind to the P_{700} - F_X core in the incorrect orientation. If the binding of PsaD does play a role in determining the correct orientation of PsaC, then it might involve the locking-in of correctly bound PsaC and the subsequent undocking of incorrectly-bound PsaC. However, this is a terribly inelegant mechanism because the incorrectly bound PsaC proteins would again

rebind correctly only 50% of the time, asymptotically approaching 100% native binding only at infinite time. There must be a different approach to the asymmetric orientation of PsaC.

Comparison of NMR solution structure of unbound PsaC with X-ray crystal structure of PS I-bound PsaC

Although PsaC is a membrane-associated protein, it is highly soluble in its unbound state. The ability to express large amounts of unbound PsaC via recombinant technology has allowed the determination of its three-dimensional solution structure by NMR spectroscopy. The presence of a high-resolution X-ray crystal structure of cyanobacterial PS I provided all the necessary structural details on the bound state of PsaC. This has made PsaC one of the very few membrane-associated proteins to have its structure solved in its unbound and membrane-associated states. It was therefore of interest that significant structural differences were found between the bound and unbound forms. The unique opportunity to compare the two structures provides insight to the conformational changes that occur during the process of assembly.

An initial NMR study indicated that PsaC is structurally related to dicluster bacterial ferredoxins [35]. Both contain two [4Fe-4S] cluster ligating motifs consisting of the consensus sequence CxxCxxCxxxCP, where C is cysteine, P is proline and x are other non-cysteine amino acids. PsaC, however, differs from dicluster ferredoxins in three important regions: a minor extension of the N-terminus of ~2 residues, a sequence insertion of 8 residues in the middle of the loop connecting the two cluster binding motifs and a C-terminal extension of 15 residues. These structural elements are presumably designed for specific interactions between PsaC and other components of PS I. In particular, the amino acids in the loop insertion are thought to be involved in ferredoxin/flavodoxin binding [36], and the C-terminal extension likely plays a role in binding PsaC to the PsaA/PsaB heterodimer [32]. The three H-bonds, which break the C_2 symmetry of the stromal binding surface, are located in the C-terminal extension.

The iron-sulfur core of unbound PsaC (PDB ID 1K0T) shows the highest similarity to dicluster bacterial ferredoxins [37]. The F_A cluster is ligated by C_{48C} , C_{51C} , C_{54C} and C_{21C} and the F_B cluster is ligated by C_{11C} , C_{14C} , C_{17C} and C_{58C} [38]. This particular arrangement of ligating Cys residues assures a fixed distance between F_A and F_B , by introducing a rigid one-turn α -helix between Cys III and Cys IV in each of the CxxCxxCxxxCP binding motifs. It

should be noted that the iron-sulfur cluster binding motifs and the clusters themselves exhibit a local pseudo- C_2 symmetry that is not apparent in the other regions of the protein.

The α -helix that connects F_B to the F_A binding site is followed by a PsaC-specific loop insertion that forms two strands of an antiparallel β -sheet connected by a turn. This structural feature is unique to PsaC when compared to other dicluster ferredoxins.

Also unique is that the N-terminus of unbound PsaC (amino acids 2–5) makes an abrupt right angle turn, bending and sliding in between the pre-C-terminus (amino acids 62–68) and the iron-sulfur core part of the protein (Fig. 7). Since the N-terminus is positioned perpendicular to the pre-C-terminus, there is a high degree of disorder around the F_A binding site. In dicluster bacterial ferredoxins, the N-terminus is positioned closer to the corresponding iron-sulfur cluster and forms an antiparallel β -sheet with the C-terminus [39]. The altered orientation of the N-terminus may be responsible for the oxygen sensitivity of unbound PsaC. The insufficient protein shielding of the F_A cluster may make it susceptible to oxidation by dioxygen, which oxidizes the bridging sulfur atoms to the S^0 state, resulting in the degradation of the cluster [33].

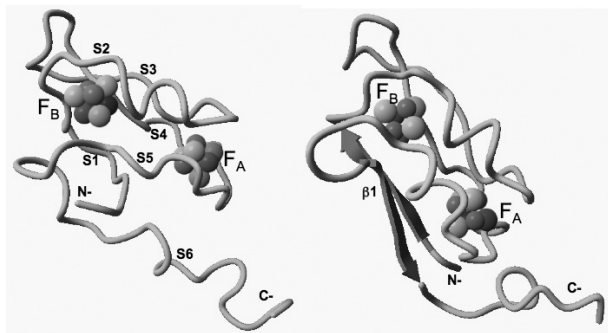


Figure 7. Structural differences between unbound PsaC (left, PDB ID: IK0T) and PS I-bound PsaC (right, PDB ID: IJB0). The protein strands are numbered S1 to S6 and the N-/C-termini are indicated. The β -sheet between the N-terminus and the pre-C-terminus in PS I-bound PsaC is denoted as β_1 .

The C-terminal extension of unbound PsaC (amino acids 68–80) is considered disordered, although it has an overall helical secondary structure. The C-terminal region does not have any packing interactions with the rest of the protein and is likely highly mobile and flexible in solution.

The crystal structure of PS I-bound PsaC shows significant structural differences in the N- and the C-terminal regions when compared to unbound PsaC [1]. The iron-sulfur core part of the protein largely remains unaltered, which is expected, given that

clusters impart a high degree of rigidity to the central protein structure. The N-terminus is positioned closer to the F_A cluster and forms an anti-parallel β -sheet with the pre-C-terminus. This conformation is significantly different from that observed in unbound PsaC, wherein the N-terminus pushes the pre-C-terminus away from the iron-sulfur core part of the protein. PS I-bound PsaC does not degrade in the presence of molecular oxygen, possibly due to adequate shielding provided to the F_A cluster by the N-terminus. The repositioned β -sheet structure between the N- and the pre-C-terminus in bound PsaC is in good agreement with the two-stranded anti-parallel arrangement that is typical of the N- and the C-termini in bacterial ferredoxins [39]. Because of the long C-terminal extension, the pre-C-terminus of PsaC is the only region that corresponds to the C-terminus of typical bacterial ferredoxins.

The actual C-terminus of PS I-bound PsaC assumes an extended conformation [1], which is strikingly different from the coiled-up structure encountered in unbound PsaC. The C-terminus is located in the binding interface of the PsaD and PsaA subunits; consequently, the high degree of structural flexibility of the C-terminus in unbound PsaC is altered to a fixed and extended form in the bound state of the protein. In contrast to PsaC, the majority of unbound PsaD does not show any extended secondary structure and a significant portion of the protein is unfolded in solution [40]. The NMR solution structure of PsaE agrees closely with that obtained in fully assembled PS I, except for some minor differences in two loop regions of the protein [41].

Implications of the Structural Differences between Unbound and Bound PsaC

A comparison between the structures of unbound and bound PsaC provides a before and after map of the conformational changes that are necessary for this membrane-associated protein to assemble properly. Because no chaperones or expenditure of ATP are involved in the binding of PsaC, the binding enthalpy between the two proteins as well as the increase in entropy from the expulsion of structural water on the binding surfaces provides the driving force for the assembly process. The major changes are the realignment of the N-terminus and the uncoiling of the C-terminus that must guide the binding of PsaC in the correct direction. Most importantly, the assembly of PsaC in the incorrect, rotated orientation on the stromal surface must be avoided.

As described previously, the binding contacts between PsaC and PsaA/PsaB can be divided into the sym-

metric ionic bonds and asymmetric H-bonds. The question arises as to which contacts are established first, given that they are likely critical for the determination of the correct orientation. In other words, what is the driving force for the formation of the initial contacts? It is given that once the first few bonds are formed between PsaC and PsaA/PsaB, the conformational dynamics of PsaC will be more restricted when compared to the unbound state and that there will be fewer routes to establish the remainder of the contacts.

Because the early stages of PsaC assembly are so critical, attempts have been made to predict the sequence of formation of the contacts between PsaC and PsaA/PsaB. Antonkine and co-workers have developed two models to explain the assembly of PsaC, based on a comparison of the structures of unbound and PS I-bound PsaC [32].

Tail-first Mechanism of PsaC Binding

This model proposes that the H-bonds between the C-terminus of PsaC and the specific pocket on PsaB are formed first, thus breaking the symmetry and determining the correct orientation at the onset of binding [32]. Once PsaC is tethered to PsaB via the C-terminus, the remaining ionic contacts are established as the protein presses down on the stromal surface, eliminating the solvent molecules at the binding interface.

This model relies strongly on the C-terminal Y80_C residue correctly locating its H-bonding partners, Q678_B and P703_B. It is within reason that the flexibility of the C-terminus might be sufficient to explore a sufficiently large conformational space so as to locate the correct H-bonding residues on PsaB. According to the tail-first mechanism, the uncoiling of the PsaC C-terminus into an extended conformation is necessary for the first committed binding step. However, it is difficult to ascertain whether the formation of a few hydrogen bonds between PsaC and PsaB provides a strong enough driving force for the uncurling of the C-terminus and correct positioning of subsequent side chains for the remainder of the docking process.

This mechanism has gained favor, mainly because it by definition precludes the possibility of PsaC binding in the wrong orientation. Computational studies, involving a geometric simulation algorithm also lend support to this model [42]. The algorithm simulates large-scale motions in proteins and attempts to provide a snapshot of the possible intermediates. Based on the conformational changes predicted by the algorithm, it was determined that the tail-first mechanism was the likely mode of PsaC binding, given that the backbone

conformation during assembly closely resembles the crystal structure of PS I-bound PsaC. It was predicted that Y80_C would be of absolute, crucial importance, since it forms most of the asymmetric H-bonds with PsaB [42].

Symmetry-first Mechanism of PsaC Binding

The alternate mode of PsaC binding involves the formation of the symmetric ionic contacts as the first step in the binding process [32]. The asymmetric H-bonds would be established subsequently to ensure the correct orientation of PsaC. The flaw with this mechanism involves the possibility of PsaC binding in the wrong C_2 -symmetric orientation. The high degree of symmetry in the Asp-Arg contacts between PsaC and PsaA/PsaB would introduce ambiguity in the orientation of PsaC on the PS I stromal surface. Were the formation of the symmetric contacts to be the first binding step, R52_C could bind either to PsaA or PsaB. Similarly, R65_C could bind to either subunit of the PS I heterodimer, with no apparent decrease in the strength of the interactions. As a result, there would exist a 50% probability that PsaC would bind in the incorrectly rotated orientation, with the F_A - F_B vector pointing towards PsaK.

This scenario would involve the breaking and reformation of ~10 ionic bonds every time incorrectly bound PsaC has to dissociate and rebind. It is extremely unlikely that nature would evolve such an energy-expensive, inelegant mechanism to bind PsaC to the PsaA/PsaB heterodimer. Soluble acceptors such as ferredoxin cannot accept electrons from PS I in the absence of PsaD and thus an incomplete stromal assembly would result in a significant loss of electrons for the carbon fixation cycle, which would adversely effect cellular metabolism. Clearly, something must prevent the symmetric region from binding first.

Heretofore Unaddressed Issues

Although these elementary models provide insight into the difficulties involved in the bioassembly of the stromal subunits, they fail to address several key issues. Both provide only a broad perspective of the binding process, without focusing on the required conformational changes in PsaC. Since PsaC is able to locate the binding surface on PsaA/PsaB without any assistance, the conformational changes themselves must unlock the driving force for binding. Thus, energy considerations are vital to understanding the stromal assembly process.

These models also do not consider structural details that are critical to the proper assembly of PsaC. Firstly, the positioning of the N-terminus in unbound PsaC, perpendicular to the C-terminus has a profound influence on the tertiary structure of the protein. The effect is to splay out strands S5 and S6 so that $K51_C$, $R52_C$ and $R65_C$ are distant from the equilibrium positions that they attain in bound PsaC (Fig. 8). The consequence is that they are completely unable to make contact with the $D568_A$, $D579_A$, $D555_B$ and $D566_B$. Simply put, this precludes PsaC docking in the symmetric regions, thus neatly solving the problem inherent in the elementary symmetry-first mechanism. The repositioning of the N-terminus at some point during the assembly process allows the strands to relax and thus orient the positively charged residues correctly.

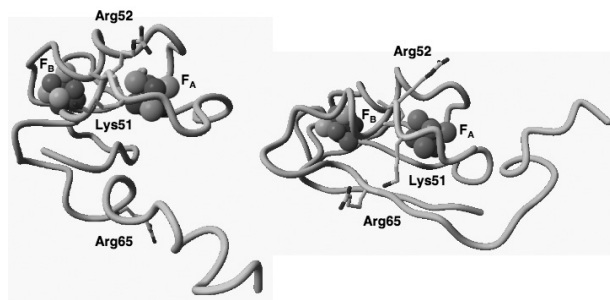


Figure 8. The positioning of the ionic bond forming residues ($K51_C$, $R52_C$ and $R65_C$) in unbound PsaC (left, PDB ID: IK0T) and PS I-bound PsaC (right, PDB ID: IJB0). The orientation of the N-terminus in unbound PsaC causes the residues to be distant from the equilibrium positions that they attain in PS I-bound PsaC.

Secondly, the presence of hydrophobic amino acids on the C-terminus of PsaC and the presence of a deep hydrophobic binding pocket on PsaB adds a further dimension to the energetics of binding. The C-terminus of PsaC contains a Gly-Leu-Ala-Tyr sequence that could participate in hydrophobic interactions with the Pro-Val-Ala-Leu sequence on PsaB. $Y80_C$ and $P703_B$, which form the asymmetric hydrogen bonds, are also located on the corresponding hydrophobic patches.

While the proposed models account for the enthalpic contribution to the Gibbs free energy due to bond formation, the entropic contribution from the fusion of hydrophobic surfaces is a more difficult undertaking. Hydrophobic residues on the surface of a protein result in the structuring of the solvent water. In an attempt to maximize freedom of the solvent, the hydrophobic surfaces of two proteins will coalesce, thus increasing the entropy of the system and making the process energetically more favorable. In principle, the C-terminus of PsaC can have hydrophobic inter-

actions with both PsaA and PsaB, thus diminishing the asymmetry introduced by the three specific H-bonds between PsaB and the C-terminus of PsaC. However, an analysis of the PS I stromal surface reveals a subtle, albeit important structural detail. Almost all the hydrophobic side chains on the PsaA stromal surface are positioned towards the interior of the membrane. This is not surprising, given that the shielding of hydrophobic surfaces from solvent molecules provides a favorable entropic contribution. However, on the corresponding PsaB stromal surface, several hydrophobic side chains are directed towards the solvent environment. Although this positioning is thermodynamically unfavorable, it may have been selected through evolution for interactions with the hydrophobic amino acids on the C-terminus of PsaC. The docking of PsaC should eliminate the solvent water molecules from the binding interface, thus increasing the entropy of the system due to the release of trapped water molecules structured around the hydrophobic side chains. Given the large surface area of the hydrophobic pocket, it is possible that the entropic contribution is significantly greater than the enthalpic contribution from the formation of the three asymmetric H-bonds between PsaB and the C-terminus of PsaC. Given the lack of specificity in hydrophobic bonds, the purpose of the three H-bonds between $T73_C/Y80_C$ and $Q678_B/K702_B/P703_B$ may simply be to steer and lock the C-terminus into its final configuration.

A Comprehensive Model for PsaC Assembly

With these considerations in mind, we propose a step-by-step model for PsaC assembly taking into account the known conformational changes as well as satisfying thermodynamic considerations.

The first committed binding step of this model would involve the anchoring of the C-terminus of PsaC (amino acids 68–80) to the specific pocket on PsaB. The uncoiling of the unstructured C-terminus would allow it to explore a large conformational space in order to locate the hydrophobic binding pocket on PsaB. Other than providing specificity, it is debatable whether the H-bonding amino acids provide a large enthalpy of binding. The entropic driving force provided by the loss of structured water in the fusion of the large hydrophobic surface on PsaB as well as the C-terminal region of PsaC is likely to be sufficiently strong to drive the binding. The absence of solvent-exposed hydrophobic side chains on PsaA would be an additional factor that determines the correct orientation of PsaC.

It is likely that the H-bonds are not formed instantly and that the hydrophobic amino acids aggregate and undergo minor realignments (twists) to maximize the hydrophobic interactions. The H-bonds between Y80_C/T73_C and PsaB would subsequently form to 'lock' the system into a thermodynamic minimum. The twisting of the C-terminus may impose considerable strain on the pre-C-terminus, given that the entire PsaC protein will trail behind the tethered C-terminus. The energy stored in the pre-C-terminal region of PsaC must be released for the system to attain thermodynamic stability. The pre-C-terminus (amino acids 64–68) would need to twist to release the strain caused by the extended C-terminus. This twisting action would position the pre-C-terminal backbone to potentially form H-bonds with the N-terminal backbone. The formation of these bonds would require the N-terminus (amino acids 2–5) to be pulled towards the F_A cluster and straighten, thereby placing it in a position to form the antiparallel β -sheet with the pre-C-terminus. The bent N-terminus may exist in a dynamic equilibrium with its straightened form (indeed, one of the 30 energy-minimized structures in the PDB file 1K0T shows a non-bent form), which would allow it to realign upon the binding of the C-terminus to the specific pocket on PsaB. The final formation of a β -sheet between the N-terminus and the pre-C-terminus would serve to stabilize this conformational change. The repositioning of the N-terminus would additionally permit the S5 and S6 strands of protein located below the F_A and F_B clusters to relax, allowing R65_C to be correctly positioned to form ionic bonds with D555_B/D566_B. The establishment of the β -sheet structure is likely responsible for PsaC attaining its final, thermodynamically stable configuration on the PS I core, and creation of new hydrogen bonds in the β -sheet would provide the driving force for PsaC to exist in an energetically favorable conformation.

It is difficult to predict the order in which the ionic contacts are formed, or if certain contacts are established only after PsaD binds, but R65_C is a good candidate to initiate the formation of the symmetric ionic contacts. The earlier flipping of the pre-C-terminus would place the side chain of R65_C very close to PsaB, and the formation of these initial ionic bonds could be critical in stabilizing PsaC on the PS I core. Either K51_C or R52_C could form the next set of contacts, although R52_C might be favored, given that PsaC-PsaA bonds might be necessary to balance PsaC on the stromal surface.

Spectroscopic evidence suggests that the environment around F_A and F_B is altered upon the binding of PsaD [26]. While this observation could be due to the clamping down of the PsaC subunit, it is also possible

that the binding of PsaD induces the tight formation of otherwise-loose ionic contacts between PsaC and PsaA/PsaB. In the latter case, it is possible that K51_C and/or R52_C are involved in the PsaD-induced bond formation, since they are part of the CxxCxxCxxCP motif that coordinates the F_A cluster. This would correlate well with the alteration in the magnetic properties of the iron-sulfur clusters in PsaC upon the binding of PsaD.

PS I-bound PsaC contains several intra-PsaC contacts that might serve to stabilize the protein during the binding process. These contacts are not observed in unbound PsaC, and it may be presumed that these are formed during the binding of PsaC and/or PsaD to the PS I core. Although the role of these intra-PsaC contacts and their sequence of formation during the binding process are difficult to predict, they should add to the stability of the bound PsaC, thereby contributing favorably to the free energy of the binding process.

The above-described model represents an attempt to add detail to previous models; it includes sequential details on the conformational changes that occur during the assembly of PsaC and it attempts to view these changes from a thermodynamic point-of-view. In this description, the N-terminus has a crucial role in the assembly process: it prevents PsaC from binding in the rotated, C_2 -symmetric orientation by misaligning the ionic bond form residues in unbound PsaC and it is also likely responsible for PsaC attaining a thermodynamic minimum by forming a β -sheet with the pre-C-terminus.

Evolutionary Considerations in the Change from a Homodimer to a Heterodimer

From a geometrical perspective, a three-dimensional surface is easiest to construct by abutting two two-dimensional surfaces. The highly protected environment at the interface of two identical protein surfaces would neatly solve the problem of shielding the electron transfer cofactors from water without requiring a highly folded three-dimensional structure such as the interior of a protein. In this regard, it is interesting that the ligands to both P₇₀₀ at the beginning, and F_X at the end of the electron transfer chain are provided by both proteins and that they are located precisely at the center of the C_2 axis of symmetry.

The symmetry of the F_X-ligating loops and the PsaC binding site on PsaA/PsaB was probably inevitable, if only because the heterodimeric core of PS I must have evolved from a homodimeric ancestor. Although a high-resolution crystal structure of a homodimeric Type I RC is not (yet) available, sequence analysis

indicates that the F_x cluster in the photosynthetic reaction centers of the photosynthetic anaerobes *Chlorobium limicola* and *Helio bacterium modestical-dum* is coordinated by Cys residues located in identical regions on each monomer subunit [43]. In this case, the system is perfectly C_2 -symmetric, since the homodimeric core is comprised of identical monomeric subunits. Subsequent gene divergence probably altered several regions of the homodimer, converting it into a heterodimer, but the environment around the redox cofactors would have been relatively unchanged, thus retaining the C_2 -symmetry of the F_x coordinating site. The purpose of the heterodimer is unknown, although it may be to provide differential binding sites for the peripheral pigment protein complexes such as *isiA* in cyanobacteria and LHCI in eukaryotic organisms such as algae and higher plants.

PsaC was probably recruited later in evolution from a pre-existing bacterial dicluster ferredoxin for the purpose of lengthening the time of charge separation between P700 and the terminal acceptors. At the time when the heterodimeric reaction center came into existence, a mechanism must have quickly evolved to lock PsaC into one of the two possible orientations. The possibility of PsaC docking in the 180° C_2 -symmetry related orientation would have been neatly circumvented in heterodimeric reaction centers by the introduction of a C-terminal extension in PsaC and the bending and movement of the N-terminus. From the point of view of energetics, the addition of the C-terminus in PsaC is a relatively small expense when compared to the energy that would be spent in utilizing helper proteins to assist in the correct binding.

Strategies to Study Stromal Assembly in Photosystem I

Although time-resolved optical spectroscopy is a relatively rapid method to monitor the binding of PsaC, the equal distances between F_x and F_B in both the native and 180° rotated orientation would likely result in equivalent forward and backward electron transfer rates. In contrast, low-temperature electron paramagnetic resonance (EPR) spectroscopy is capable of detecting minor changes in the environment surrounding the iron-sulfur clusters in PsaC. Site-directed mutagenesis offers the opportunity to study the role of each individual binding contact on PsaC. For instance, a variant of PsaC in which $Y80_C$ is converted into an alanine residue, which is less hydrophobic and lacks the H-bond forming side-chain, would be useful in understanding its role in the

binding of the C-terminus of PsaC. If the formation of H-bonds between $Y80_C$ and PsaB are a critical part of the recognition mechanism, the variant PsaC should not bind to PS I. However, if the fusion of the hydrophobic surfaces on PsaC and PsaB were the driving force behind the binding, the substitution of $Y80_C$ with an Ala residue would not have a significant impact on the assembly of PsaC. The N- and C-termini of PsaC could also be modified to better understand their roles in the assembly process. The deletion of the C-terminus would result in the loss of the hydrophobic contacts and the specific H-bonds with PsaB, which might prevent PsaC from docking on the PS I core. A PsaC variant that lacks both the N- and the C-termini would be devoid of the structural features that prevent PsaC from docking in the 180° rotated orientation. In principle, this variant could bind to the PS I core in both orientations. Both the correct and incorrect orientation of bound PsaC should exhibit identical charge-recombination kinetics and magnetic properties, rendering evidence of a rotated C_2 -symmetric orientation difficult to attain. However, because PsaD is only able to bind to the correctly oriented PsaC protein, the EPR spectrum should be an admixture of the PsaC-only spectrum and the PsaC/PsaD spectrum. A detailed analysis by computer simulation of the two spectra should allow both the correctly and incorrectly oriented PsaC protein to be measured. A crystal structure of PS I-rotated PsaC might be required to provide indisputable evidence for the existence of such a complex.

Other techniques that can be used to monitor the binding of PsaC include site-directed spin labeling (SDSL) and isothermal microcalorimetry (ITC). SDSL involves the covalent linkage of an organic molecule containing a stable nitroxide radical with the protein via disulfide bonds. The magnetic environment of the protein-bound spin label is highly sensitive to the surrounding protein matrix [44, 45] and if the labeling sites are properly chosen, SDSL can provide a direct glimpse of incorrectly bound PsaC. ITC records the heat flow and measures thermodynamic parameters such as the change in enthalpy and Gibbs free energy during binding [46].

Conclusions

The assembly of multi-subunit membrane proteins is not well understood due to the difficulty involved in isolating intermediates of these complexes and the lack of available experimental strategies to investigate the details of binding. However, it is essential to understand the assembly of such complexes, as they are often involved in critical metabolic processes. Any

disruption in the assembly would be detrimental to cellular metabolism and, as a result, it is important to understand the design principles of the assembly process as well as the factors that could lead to incorrect assembly. The rationale and experimental techniques demonstrated in the photosynthetic model can be extended to any biological system. The availability of a high-resolution crystal structure is critical, since it provides a clear insight into the assembly when compared to sequence analysis. Although the presence of redox cofactors in PS I facilitates spectroscopic analyses, techniques such as SDSL and ITC can also be employed in biological systems that do not participate in electron transfer reactions.

Acknowledgements. Funding for this work was provided by grants from the National Science Foundation (MCB-0519743) and the United States Department of Energy (DE-FG-02-98-ER20314).

- 1 Jordan, P., Fromme, P., Witt, H. T., Klukas, O., Saenger, W. and Krauss, N. (2001) Three-dimensional structure of cyanobacterial Photosystem I at 2.5 Å resolution. *Nature* 411, 909–917.
- 2 Setif, P. (2001) Ferredoxin and flavodoxin reduction by Photosystem I. *Biochim. Biophys. Acta* 1507, 161–179.
- 3 Setif, P., Fischer, N., Lagoutte, B., Bottin, H. and Rochaix, J. D. (2002) The ferredoxin docking site of Photosystem I. *Biochim. Biophys. Acta* 1555, 204–209.
- 4 Fromme, P. and Grotjohann, I. (2007) Structural analysis of cyanobacterial Photosystem I. In: *Photosystem I, The Light-Driven Plastocyanin: Ferredoxin Oxidoreductase*, pp. 47–69, Golbeck, J. H. (ed.), Springer, Dordrecht.
- 5 Chitnis, V. P. and Chitnis, P. R. (1993) PsaL subunit is required for the formation of Photosystem I trimers in the cyanobacterium *Synechocystis* sp. PCC 6803. *FEBS Lett.* 336, 330–334.
- 6 Chitnis, V. P., Xu, Q., Yu, L., Golbeck, J. H., Nakamoto, H., Xie, D. L. and Chitnis, P. R. (1993) Targeted inactivation of the gene *psaL* encoding a subunit of Photosystem I of the cyanobacterium *Synechocystis* sp. PCC 6803. *J. Biol. Chem.* 268, 11678–11684.
- 7 Schluchter, W. M., Shen, G., Zhao, J. and Bryant, D. A. (1996) Characterization of *psaI* and *psaL* mutants of *Synechococcus* sp. strain PCC 7002: a new model for state transitions in cyanobacteria. *Photochem. Photobiol.* 64, 53–66.
- 8 Xu, Q., Hoppe, D., Chitnis, V. P., Odom, W. R., Guikema, J. A. and Chitnis, P. R. (1995) Mutational analysis of Photosystem I polypeptides in the cyanobacterium *Synechocystis* sp. PCC 6803. Targeted inactivation of *psaI* reveals the function of *psaI* in the structural organization of *psaL*. *J. Biol. Chem.* 270, 16243–16250.
- 9 Brettel, K. (1997) Electron transfer and arrangement of the redox cofactors in Photosystem I. *Biochim. Biophys. Acta* 1318, 322–373.
- 10 Fish, L. E., Kuck, U. and Bogorad, L. (1985) Two partially homologous adjacent light-inducible maize chloroplast genes encoding polypeptides of the P700 chlorophyll a-protein complex of Photosystem I. *J. Biol. Chem.* 260, 1413–1421.
- 11 Vassiliev, I. R., Jung, Y. S., Smart, L. B., Schulz, R., McIntosh, L. and Golbeck, J. H. (1995) A mixed-ligand iron-sulfur cluster (C556SPsaB or C565SPsaB) in the Fx-binding site leads to a decreased quantum efficiency of electron transfer in Photosystem I. *Biophys. J.* 69, 1544–1553.
- 12 Hallahan, B., Purton, S., Ivison, A., Wright, D. and Evans, M. C. W. (1995) Analysis of the proposed FeSx binding region of Photosystem I by site directed mutation of PsaA of *Chlamydomonas reinhardtii*. *Photosynth. Res.* 46, 257–264.
- 13 Watanabe, T., Kobayashi, M., Hongu, A., Nakazato, M. and Hiyama, T. (1985) Evidence that a chlorophyll a' dimer constitutes the photochemical reaction centre I (P700) in photosynthetic apparatus. *FEBS Lett.* 235, 252–256.
- 14 Holzwarth, A. R., Müller, M. G., Niklas, J. and Lubitz, W. (2006) Ultrafast transient absorption studies on Photosystem I reaction centers from *Chlamydomonas reinhardtii*. 2: Mutations near the P700 reaction center chlorophylls provide new insight into the nature of the primary electron donor. *Biophys. J.* 90, 552–565.
- 15 Cohen, R. O., Shen, G., Golbeck, J. H., Xu, W., Chitnis, P., Valieva, A., van der Est, A., Pushkar, Y. N. and Stehlík, D. (2004) Evidence for asymmetric electron transfer in cyanobacterial Photosystem I: An analysis of a methionine to leucine mutation of the ligand to the primary electron acceptor A0. *Biochemistry* 43, 4741–4754.
- 16 Xu, W., Chitnis, P. R., Valieva, A., van der Est, A., Brettel, K., Guergova-Kuras, M., Pushkar, Y. N., Zech, S. G., Stehlík, D., Shen, G., Zybaiov, B. and Golbeck, J. H. (2003) Electron transfer in cyanobacterial Photosystem I: II. Determination of forward electron transfer rates of site-directed mutants in a putative electron transfer pathway from A0 through A1 to FX. *J. Biol. Chem.* 278, 27876–27887.
- 17 Ramesh, V. M., Gibasiewicz, K., Lin, S., Bingham, S. E. and Webber, A. N. (2004) Bidirectional electron transfer in Photosystem I: Accumulation of A0- in A-side or B-side mutants of the axial ligand to chlorophyll A0. *Biochemistry* 43, 1369–1375.
- 18 Guergova-Kuras, M., Boudreux, B., Joliot, A., Joliot, P. and Redding, K. (2001) Evidence of two active branches for electron transfer in Photosystem I. *Proc. Natl. Acad. Sci. USA* 98, 4437–4442.
- 19 Muhiuddin, I. P., Heathcote, P., Carter, S., Purton, S., Rigby, S. E. J. and Evans, M. C. W. (2001) Evidence from time resolved studies of the P700+A1- radical pair for photosynthetic electron transfer on both the PsaA and PsaB branches of the Photosystem I reaction centre. *FEBS Lett.* 503, 56–60.
- 20 Parrett, K. G., Mehari, T., Warren, P. G. and Golbeck, J. H. (1989) Purification and properties of the intact P700 and Fx-containing Photosystem I core protein. *Biochim. Biophys. Acta* 973, 324–332.
- 21 Zhao, J. D., Warren, P. V., Li, N., Bryant, D. A. and Golbeck, J. H. (1990) Reconstitution of electron transport in Photosystem I with PsaC and PsaD proteins expressed in *Escherichia coli*. *FEBS Lett.* 276, 175–180.
- 22 Zhao, J., Snyder, W. B., Muhlenhoff, U., Rhiel, E., Warren, P. V., Golbeck, J. H. and Bryant, D. A. (1993) Cloning and characterization of the *psaE* gene of the cyanobacterium *Synechococcus* sp. PCC 7002: characterization of a *psaE* mutant and overproduction of the protein in *Escherichia coli*. *Mol. Microbiol.* 9, 183–194.
- 23 Mehari, T., Parrett, K. G., Warren, P. V. and Golbeck, J. H. (1991) Reconstitution of the iron-sulfur clusters in the isolated FA/FB protein: EPR spectral characterization of same-species and cross-species Photosystem I complexes. *Biochim. Biophys. Acta* 1056, 139–148.
- 24 Parrett, K. G., Mehari, T. and Golbeck, J. H. (1990) Resolution and Reconstitution of the cyanobacterial Photosystem I complex. *Biochim. Biophys. Acta* 1015, 341–352.
- 25 Shen, G., Zhao, J., Reimer, S. K., Antonkine, M. L., Cai, Q., Weiland, S. M., Golbeck, J. H. and Bryant, D. A. (2002) Assembly of Photosystem I. Inactivation of the rubA gene encoding a membrane-associated rubredoxin in the cyanobacterium *Synechococcus* sp. PCC 7002 causes a loss of Photosystem I activity. *J. Biol. Chem.* 277, 20343–20354.
- 26 Li, N., Zhao, J. D., Warren, P. V., Warden, J. T., Bryant, D. A. and Golbeck, J. H. (1991) PsaD is required for the stable binding of PsaC to the Photosystem I core protein of *Synechococcus* sp. PCC 6301. *Biochemistry* 30, 7863–7872.
- 27 Yu, J., Smart, L. B., Jung, Y. S., Golbeck, J. and McIntosh, L. (1995) Absence of PsaC subunit allows assembly of Photo-

system I core but prevents the binding of PsaD and PsaE in *Synechocystis* sp. PCC 6803. *Plant Mol. Biol.* 29, 331–342.

28 Chitnis, V. P., Jung, Y. S., Albee, L., Golbeck, J. H. and Chitnis, P. R. (1996) Mutational analysis of Photosystem I polypeptides. Role of PsaD and the lysyl 106 residue in the reductase activity of the Photosystem I. *J. Biol. Chem.* 271, 11772–11780.

29 Barth, P., Lagouette, B. and Setif, P. (1998) Ferredoxin reduction by Photosystem I from *Synechocystis* sp. PCC 6803: Toward an understanding of the respective roles of subunits PsaD and PsaE in ferredoxin binding. *Biochemistry* 37, 16233–16241.

30 Yu, L., Zhao, J., Muhlenhoff, U., Bryant, D. A. and Golbeck, J. H. (1993) PsaE is required for *in vivo* cyclic electron transfer around Photosystem I in the cyanobacterium *Synechococcus* sp. PCC 7002. *Plant Physiol.* 103, 171–180.

31 Cohen, Y., Chitnis, V. P., Nechushtai, R. and Chitnis, P. R. (1993) Stable assembly of PsaE into cyanobacterial photosynthetic membranes is dependent on the presence of other accessory subunits of Photosystem I. *Plant Mol. Biol.* 23, 895–900.

32 Antonkine, M. L., Jordan, P., Fromme, P., Krauss, N., Golbeck, J. H. and Stehlík, D. (2003) Assembly of protein subunits within the stromal ridge of Photosystem I. Structural changes between unbound and sequentially PS I-bound polypeptides and correlated changes of the magnetic properties of the terminal iron sulfur clusters. *J. Mol. Biol.* 327, 671–697.

33 Golbeck, J. H., Lien, S. and San Pietro, A. (1977) Isolation and characterization of a subchloroplast particle enriched in iron-sulfur protein and P700. *Arch. Biochem. Biophys.* 178, 140–150.

34 Moser, C. C., Keske, J. M., Warncke, K., Farid, R. S. and Dutton P. L. (1992) Nature of biological electron transfer. *Nature* 355, 796–802.

35 Bentrop, D., Bertini, I., Luchinat, C., Nitschke, W. and Mühlenhoff, U. (1997) Characterization of the unbound 2[Fe4S4]-ferredoxin-like Photosystem I subunit PsaC from the cyanobacterium *Synechococcus elongatus*. *Biochemistry* 36, 13629–13637.

36 Setif, P. (2007) Electron transfer from the bound iron-sulfur clusters to ferredoxin/flavodoxin: Kinetic and structural properties of ferredoxin/flavodoxin reduction by Photosystem I. In: *Photosystem I, The Light-Driven Plastocyanin: Ferredoxin Oxidoreductase*, pp. 439–454, Golbeck, J. H. (ed.), Springer, Dordrecht.

37 Antonkine, M. L., Liu, G., Bentrop, D., Bryant, D. A., Bertini, I., Luchinat, C., Golbeck, J. H. and Stehlík, D. (2002) Solution structure of the unbound, oxidized Photosystem I subunit PsaC, containing [4Fe-4S] clusters FA and FBs: a conformational change occurs upon binding to Photosystem I. *J. Biol. Inorg. Chem.* 7, 461–472.

38 Vassiliev, I. R., Antonkine, M. L. and Golbeck, J. H. (2001) Iron-sulfur clusters in type I reaction centers. *Biochim. Biophys. Acta* 1507, 139–160.

39 Sticht, H. and Rösch, P. (1998) The structure of iron-sulfur proteins. *Prog. Biophys. Mol. Biol.* 70, 95–136.

40 Xia, Z., Broadhurst, R. W., Laue, E. D., Bryant, D. A., Golbeck, J. H. and Bendall, D. S. (1998) Structure and properties in solution of PsaD, an extrinsic polypeptide of Photosystem I. *Eur. J. Biochem.* 255, 309–316.

41 Falzone, C. J., Kao, Y. H., Zhao, J., Bryant, D. A. and Lecomte, J. T. (1994) Three-dimensional solution structure of PsaE from the cyanobacterium *Synechococcus* sp. strain PCC 7002, a Photosystem I protein that shows structural homology with SH3 domains. *Biochemistry* 33, 6052–6062.

42 Jolley, C. C., Wells, S. A., Hespenheide, B. M., Thorpe, M. F. and Fromme, P. (2006) Docking of Photosystem I subunit C using a constrained geometric simulation. *J. Am. Chem. Soc.* 128, 8803–8812.

43 Büttner, M., Xie, D. L., Nelson, H., Pinther, W., Hauska, G. and Nelson, N. (1992) Photosynthetic reaction center genes in green sulfur bacteria and in Photosystem I are related. *Proc. Natl. Acad. Sci. USA.* 89, 8135–8139.

44 Hubbell, W. L., Cafiso, D. S. and Altenbach, C. (2000) Identifying conformational changes with site-directed spin labeling. *Nat. Struct. Biol.* 7, 735–739.

45 Fanucci, G. E. and Cafiso, D. S. (2006) Recent advances and applications of site-directed spin labeling. *Curr. Opin. Struct. Biol.* 16, 644–653.

46 Doyle, M. L. (1997) Characterization of binding interactions by isothermal titration calorimetry. *Curr. Opin. Biotechnol.* 8, 31–35.